

Retraction

Retracted: Research on Nonline-of-Sight Positioning Method of Intelligent Mobile Terminal Based on Intelligent Monitoring Architecture of Multimedia Sensor Network

Advances in Multimedia

Received 15 August 2023; Accepted 15 August 2023; Published 16 August 2023

Copyright © 2023 Advances in Multimedia. This is an open access article distributed under the Creative Commons Attribution License, which permits unrestricted use, distribution, and reproduction in any medium, provided the original work is properly cited.

This article has been retracted by Hindawi following an investigation undertaken by the publisher [1]. This investigation has uncovered evidence of one or more of the following indicators of systematic manipulation of the publication process:

- (1) Discrepancies in scope
- (2) Discrepancies in the description of the research reported
- (3) Discrepancies between the availability of data and the research described
- (4) Inappropriate citations
- (5) Incoherent, meaningless and/or irrelevant content included in the article
- (6) Peer-review manipulation

The presence of these indicators undermines our confidence in the integrity of the article's content and we cannot, therefore, vouch for its reliability. Please note that this notice is intended solely to alert readers that the content of this article is unreliable. We have not investigated whether authors were aware of or involved in the systematic manipulation of the publication process.

Wiley and Hindawi regrets that the usual quality checks did not identify these issues before publication and have since put additional measures in place to safeguard research integrity.

We wish to credit our own Research Integrity and Research Publishing teams and anonymous and named external researchers and research integrity experts for contributing to this investigation.

The corresponding author, as the representative of all authors, has been given the opportunity to register their

agreement or disagreement to this retraction. We have kept a record of any response received.

References

- [1] J. Liu, "Research on Nonline-of-Sight Positioning Method of Intelligent Mobile Terminal Based on Intelligent Monitoring Architecture of Multimedia Sensor Network," *Advances in Multimedia*, vol. 2021, Article ID 6008458, 9 pages, 2021.

Research Article

Research on Nonline-of-Sight Positioning Method of Intelligent Mobile Terminal Based on Intelligent Monitoring Architecture of Multimedia Sensor Network

Jianjun Liu 

School of Information Science and Engineering of Hebei North University, Zhangjiakou, Hebei 000730, China

Correspondence should be addressed to Jianjun Liu; liujj@hebeinu.edu.cn

Received 13 July 2021; Accepted 23 July 2021; Published 21 October 2021

Academic Editor: Zhendong Mu

Copyright © 2021 Jianjun Liu. This is an open access article distributed under the Creative Commons Attribution License, which permits unrestricted use, distribution, and reproduction in any medium, provided the original work is properly cited.

With the continuous development of social economy, information resources have become more and more valued resources. Based on the intelligent monitoring architecture of the multimedia sensor network, this article proposes a nonlinear-of-sight positioning method that can fit the characteristics of autonomous movement for the object of intelligent terminal, that is, first draw the corresponding position trajectory according to the speed attribute of the node. On this basis, according to the relative position trajectory and radio frequency signal positioning, the two-by-two positioning of position and direction is comprehensively realized, and the positioning result is obtained; the positioning accuracy is evaluated according to the positioning of the radio frequency signal, and the false positioning result of the distorted radio frequency signal is stripped out to reduce the error influences. Practical results show that the method is effective and can meet the needs of positioning accuracy.

1. Introduction

With the development of society and economy, information resources have become more and more valued resources, and location information has become more and more important. For example, food, clothing, housing, and transportation are inseparable, and takeaways need to specify specific locations [1]. In the world of intelligent connection of all things, autonomously connected mobile nodes have been more and more used in areas such as manual input or GPS, BEIDOU receiver for position positioning. However, this part will be restricted by the module, and the positioning accuracy will be insufficient due to the influence of non-viewing distance factors. However, in wireless sensor networks, the main research object is static nodes rather than mobile nodes, so this part needs to focus on [2, 3].

The positioning method for mobile nodes can generally be direct radio frequency positioning, that is, through target

recognition and data fusion, it can distinguish moving people, moving vehicles, etc., such as using WiFi, mobile phone signaling data can achieve location positioning [4–6]. In recent years, GPS positioning may not be able to achieve fast and accurate positioning. With distributed computing technology or wireless signaling technology, positioning based on WiFi and mobile phone signals has become a new way and new means of location information acquisition [7–10]. The focus is on the avoidance and handling of a large number of obstacles, because this may lead to a decrease in the accuracy of the position accuracy.

Based on the above limitations, this article relies on the intelligent monitoring architecture of the multimedia sensor network, takes the mobile node as the entry point, traces the displacement speed, outlines the corresponding action trajectory, and then uses the auxiliary radio frequency signal to comprehensively judge the position result, aiming to improve the positioning accuracy.

2. Design of Intelligent Monitoring Architecture for Multimedia Sensor Network

2.1. Multimedia Monitoring Network Based on Low Power Consumption Design. Aiming at the intelligent monitoring architecture of the multimedia sensor network, this paper combines video, infrared, and other diversified sensor device data to obtain the characteristics of related targets from multiple angles and aspects, forming a diversified feature space dimension, which is more conducive to target identification and extraction [11]. The specific fusion is shown in Figure 1. Through the fusion of image, video, and other data, the characteristics of the target are associated, and the target characteristics are extracted into a vector file for recognition of the target characteristics.

The corresponding data collected by all sensor devices (such as remote sensing devices) are sorted, processed, analyzed, and combined in the sensor network. As for multimedia monitoring networks, streaming media data processing has higher requirements on the accuracy of data collection and data processing capabilities. At present, the main body is the data fusion of graphics and images, and other sensor networks involve comprehensive time fusion of data. In particular, the corresponding feature fusion recognition of the target is based on the joint associated features after classification to perform the corresponding recognition processing.

The processing and analysis of the target image mainly involve video data, audio data, and basic data. Among them, the basic data mainly include infrared sensor equipment and traditional telemetry data. Usually, the basic data flow is relatively small. Compared with the basic data, audio and video data are relatively large and redundant and need to be collected, processed, sorted, and analyzed by means and hardware devices with strong computing capabilities to achieve data compression and feature processing.

2.2. Wireless Network Design. On the basis of the first section above, this article attempts to use WiFi to provide data communication services at the control layer with large data streams such as video and audio, so as to realize the networking and control of basic sensors. This method can be used for large-scale farm planting. For a large number of planting areas, a large number of sensors are deployed, which is conducive to real-time monitoring of geological disasters and crop growth. It not only improves efficiency but also achieves effective monitoring and realizes the practical application of "Internet +" [12, 13].

The fusion center gathers data collected by all multimedia sensor nodes and presents real-time monitoring to users through a visual interface. Users can control and process any terminal through a large-screen visual interface.

2.3. Network Application Design. When the wireless network is set up, the covered place will form a wireless network. The sensor will send corresponding information back to the master node through transmission. When the master node receives the corresponding sensor network message, it will

start the corresponding emergency treatment process and locate the specific location of the abnormality. At the same time, data, audio, video, etc., of abnormal locations need to be stored first, and then the corresponding feature codes are extracted and transmitted to the fusion center through the transmission signal and then transmitted back to the mobile terminal to realize abnormal alarm reminders [14, 15].

The mobile node uses the speed information it can obtain to estimate the change of its own pose state over time, so as to obtain its own motion trajectory, that is, the relative positioning trajectory.

According to the corresponding displacement speed information to judge the change of the pose state, thereby obtaining its own motion trajectory and realizing relative positioning, then the corresponding state and speed information are specifically obtained for calculation with the following formula:

$$\begin{cases} X_h(k) = X_h(k-1) + \begin{bmatrix} \cos(\alpha_h(k-1)) \\ \sin(\alpha_h(k-1)) \end{bmatrix} \cdot V(k) \cdot \Delta T, \\ \alpha_h(k) = \alpha_h(k-1) + \theta(k). \end{cases} \quad (1)$$

The comprehensive positioning technology needs to measure both the direction and the speed of the mobile node. If the initial position and movement direction of the node are known, the positioning trajectory in the ideal state should be completely consistent with the actual movement trajectory without the influence of other external factors. However, it cannot be ignored that errors are inevitable, and the accuracy of positioning will eventually be affected by corresponding angle errors, speed errors, etc., resulting in a certain deviation in positioning accuracy.

2.4. MSNIMA Algorithm. In response to the aforementioned needs and problems, this article proposes the MSNIMA algorithm, which is mainly composed of the following steps:

- (a) Initial initialization: at this stage, set the corresponding initialization value, and at the same time, set the initial state of the relative positioning, as shown in the following formula:

$$\begin{cases} X_h(0) = [0 \ 0]^T, \\ \alpha_h(0) = 0. \end{cases} \quad (2)$$

It should be noted that the initialized position can also be set to other values, which is only a certain measurement reference and does not represent practical significance. MSNIMA only makes comprehensive use of relative positioning, not absolute positioning.

- (b) Location evaluation: on the basis of initialization, the historical results of relative positioning are evaluated with algorithms, the current position information is obtained, and the accuracy of the radio frequency positioning is directly used for calculation.

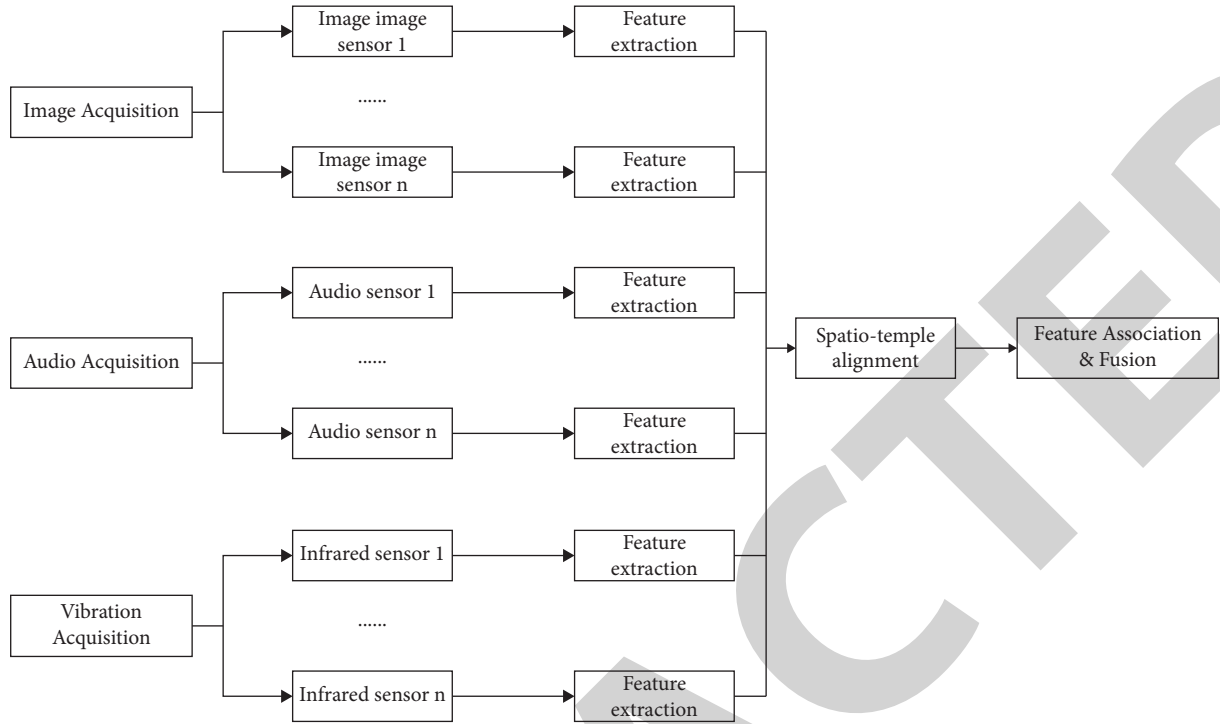


FIGURE 1: Heterogeneous sensor feature fusion process.

(c) The threshold is determined, and the corresponding threshold and historical record length are set.

The specific process is as follows:

(1) Use formula (3) to express the last N effective radio frequency positioning results:

$$Y_r^{kN} = [X_r(k-N), X_r(k-N+1) \dots X_r(k-1)]. \quad (3)$$

(2) The relative positioning result of translation and the result of radio frequency positioning make the center of the two as the origin, and the coordinate matrix after translation is expressed by the following equations:

$$\begin{aligned} CY_r^{kN} &= [CX_r(k-N)CX_r(k-N+1) \dots CX_r(k-1)] \\ &= [X_r(k-N) - C_r^{kN}(X_r(k-N+1)) - C_r^{kN} \dots X_r(k-1) - C_r^{kN}], \end{aligned} \quad (4)$$

$$\begin{aligned} CY_h^{kN} &= [CX_h(k-N)CX_h(k-N+1) \dots CX_h(k-1)] \\ &= [X_h(k-N) - C_h^{kN}(X_h(k-N+1)) - C_h^{kN} \dots X_h(k-1) - C_h^{kN}], \end{aligned} \quad (5)$$

$$C_r^{kN} = \frac{1}{N} \cdot \sum_{i=0}^{N-1} X_r(k-N+i), \quad (6)$$

$$C_h^{kN} = \frac{1}{N} \cdot \sum_{i=0}^{N-1} X_h(k-N+i). \quad (7)$$

- (3) Rotate the relative positioning result around the origin to minimize the difference with the RF positioning result. The coordinates obtained by rotating

the relative positioning result around the center θ can be represented by the following equations:

$$RCY_h^{kN}(\theta) = [RCX_h(k-N, \theta), RCX_h(k-N+1, \theta) \dots RCX_h(k-1, \theta)] = \begin{bmatrix} \cos(\theta) & -\sin(\theta) \\ \sin(\theta) & \cos(\theta) \end{bmatrix} \cdot CY_h^{kN}. \quad (8)$$

Rotating to minimize the difference in positioning results means looking for the following θ :

$$\theta_{\min}(k) = \min_{\theta \in [0, 2\pi)} \text{diff}(\theta), \quad (9)$$

$$\text{diff}(\theta) = \|RCY_h^{kN}(\theta) - CY_r^{kN}\|^2 = \sum_{i=0}^{N-1} \|RCX_h(k-N+i, \theta) - CX_r(k-N+i)\|^2. \quad (10)$$

Obviously, $\text{diff}(\theta)$ is a continuous differentiable function of θ , and its derivative is also continuous and differentiable, and it is a function with a period of 2π . It can be obtained in a period by solving $[-0.5\pi \ 1.5\pi]$ taking the minimum value of θ as

$$\theta_{\min} = \begin{cases} 0 & (a = 0, b = 0) \\ -0.5\pi & (a = 0, b > 0) \\ 0.5\pi & (a = 0, b < 0) \\ \arctan(b/a) & (a < 0) \\ \arg \tan(b/a) + \pi & (a > 0) \end{cases}, \quad (11)$$

$$\begin{cases} a = \langle CY_h^{kN}, CY_r^{kN} \rangle, \\ b = \langle CY_h^{kN}, \begin{bmatrix} 0 & 1 \\ -1 & 0 \end{bmatrix} CY_r^{kN} \rangle. \end{cases} \quad (12)$$

It should be noted that $a = 0$ and $b = 0$ will only occur when the node is not moving for a long time. In this case, although any θ can make $\text{diff}(\theta)$ take the minimum value, this article is in the actual calculation process, the value is 0.

- (4) After $\theta_{\min}(k)$ getting' shift the relative positioning trajectory again so that the center is the original RF positioning center, and the final positioning result and the speed direction can be obtained as follows:

$$X_{\text{final}}(k) = \begin{bmatrix} \cos(\theta_{\min}(k)) & -\sin(\theta_{\min}(k)) \\ \sin(\theta_{\min}(k)) & \cos(\theta_{\min}(k)) \end{bmatrix} \cdot (X_h(k) - C_h^{kN}) + C_r^{kN}, \quad (13)$$

$$\alpha_{\text{final}}(k) = \alpha_h(k) + \theta_{\min}(k). \quad (14)$$

It can be seen from Figure 2 that while obtaining the positioning position, an estimate of the radio frequency positioning accuracy can also be obtained,

$$\bar{P} = \sqrt{\frac{\text{diff}(\theta_{\min})}{N}}. \quad (15)$$

The determination of the threshold η should meet two conditions: first, it can distinguish severely distorted radio frequency positioning results; second, it should help nodes recover from the cumulative error of relative positioning. Obviously, when the radio frequency positioning accuracy p is higher, the threshold η should be smaller; the lower the

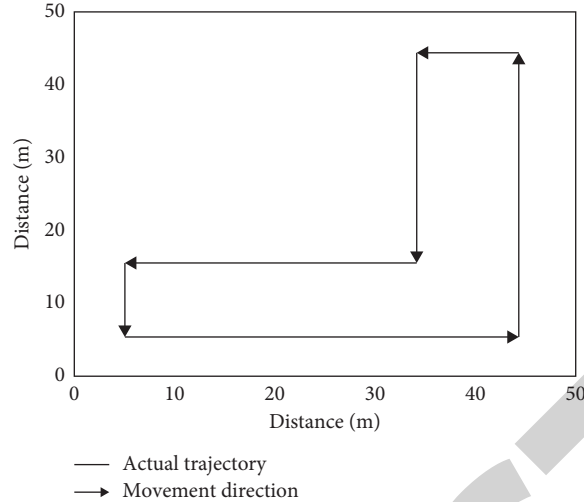


FIGURE 2: The relationship between the mean value of LOS error μ_N and RMSE.

accuracy p is, the threshold η should be larger to effectively distinguish the distortion positioning results.

The threshold used in this paper is shown in the following formula:

$$\eta = \begin{cases} \sqrt{\frac{\text{diff}(\theta)}{N}} \cdot (1.5 + 0.07N_{kN}), N_{kN} < 0.6N; \\ +\infty, N_{kN} \geq 0.6N. \end{cases} \quad (16)$$

Similar to the threshold η , the value of N cannot be set to a fixed value. When the accuracy p is smaller, N should also be smaller to minimize the impact of accumulated errors. Conversely, when p is larger, N should also be larger, in order to minimize the influence of radio frequency positioning errors and obtain high-precision pose information.

The value of N in this paper is shown in the following formula:

$$N = \max\{[a_N \bar{p} + b_N], N_{\min}\}. \quad (17)$$

In the formula, the value of a_N is 13, the value of b_N is 1, the value of N_{\min} is 10, and the value of $[x(k), y(k)]$ is rounded to x .

3. Simulation Results and Performance Analysis

3.1. Simulation Model. First, set up the simulation environment for the experiment. Within a square range of 50 m for a mobile node, move counterclockwise along the black tip, as shown in Figure 3. The displacement speed is 1 m/s, and the time interval is 0.5 s for mobile positioning, and finally, the measurement of the mobile position is realized.

In the specific simulation experiment, this article chooses the MSNIMA method, and the positioning method chooses DTN as the radio frequency signal positioning method, because it applies to the three strongest signal nodes of all signals to achieve positioning, which is more accurate and relatively accurate. The signal strength is shown in the following formulas:

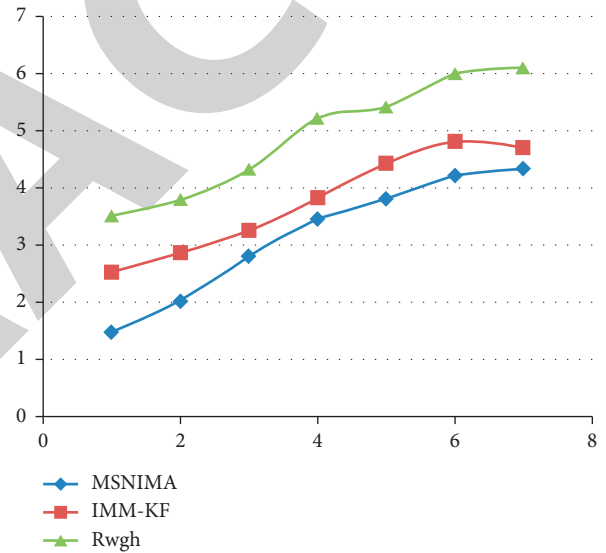


FIGURE 3: Simulation environment.

$$\text{RSSI}_{\text{dBm}}(d) \sim N(P_{\text{dBm}}(d), \sigma_{\text{dB}}^2), \quad (18)$$

$$P_{\text{dBm}}(d) = P_{\text{dBm}}(d_0) - 10n \lg\left(\frac{d}{d_0}\right). \quad (19)$$

In the formula, dBm and dB are used to indicate the unit, $[\hat{x}(k), \hat{y}(k)]$ indicates the reference distance, and $b \sim N(\mu_N, \sigma_N^2)$ is used to indicate the RF signal strength at μ_N , which is determined by the external environment.

Among them, for the influence of obstacles on the positioning accuracy, this paper simulates the attenuation of nodes, and the specific calculation is shown in the following formula:

$$\text{RSSI}_{\text{dBm}}(d) \sim N(P_{\text{dBm}}(d) - \tau_{\text{dB}} \sigma_{\text{dB}}^2). \quad (20)$$

From this, the estimated μ_N for d can be obtained as

$$\begin{aligned}\bar{d} &= d_0 \cdot 10^{\frac{(P_{dBm}(d_0) - \text{RSSI}_{dBm}(d) + \tau_{dB})}{10n}} \\ &= d_0 \cdot 10^{\frac{(P_{dBm}(d_0) - P_{dBm}(d) + \tau_{dB})}{10n}} \cdot 10^{\frac{(P_{dBm}(d) - \text{RSSI}_{dBm}(d) + \tau_{dB})}{10n}}.\end{aligned}\quad (21)$$

Substituting formula (20) into (22) can obtain the following formula:

$$\bar{d} = d \cdot 10^{u(d)}, \quad (22)$$

$$u(d) = \frac{P_{dBm}(d) - \text{RSSI}_{dBm}(d) + \tau_{dB}}{10n}. \quad (23)$$

From equations (20) and (24), we know that $u(d)$ obeys the following Gaussian distribution:

$$u(d) \sim N\left(\frac{\tau_{dB}}{10n}, \text{cov}\right), \text{cov} = \frac{\sigma_{dB}^2}{(10n)^2}. \quad (24)$$

When there is no obstacle between the mobile node and the beacon node, $\mu_N = 2$ is zero; otherwise, it is the corresponding fading value.

3.2. Result Analysis. According to the setting of the abovementioned simulation environment, 7 signal nodes, 2 obstacles, and 1 unknown node are arranged in the range, and a uniform motion of 1 m/s is realized in this area. The conversion probability can be defined by the following formula:

$$\psi = \begin{bmatrix} 0.9 & 0.1 \\ 0.1 & 0.9 \end{bmatrix}. \quad (25)$$

By comparing the MSNIMA algorithm with the IMM-KF algorithm and the Rwgh algorithm, obtaining the corresponding experimental data in the same simulation environment and evaluating the accuracy of the corresponding algorithm through the root mean square error are shown in the following formula:

$$\text{RMES} = \sqrt{\frac{1}{K} \sum_{k=1}^K (x(k) - \hat{x}(k))^2 + (y(k) - \hat{y}(k))^2}, \quad (26)$$

where $[x(k), y(k)]$ is the real position of the unknown node at time k , and $[\hat{x}(k), \hat{y}(k)]$ is the simulated position of the unknown node at time k .

3.2.1. Nonline-of-Sight Error. As shown in Figure 2, in this simulation experiment, the relationship between the LOS error value and the RMSE is mainly studied. The noise obeys the Gaussian distribution. From the results, as μ_N increases, the RMSE values of all algorithms increase. But the MSNIMA algorithm in this paper has more obvious advantages, and the positioning accuracy is relatively higher.

As shown in Figure 4, this result shows that when the LOS error value is 2, the noise measurement obeys the

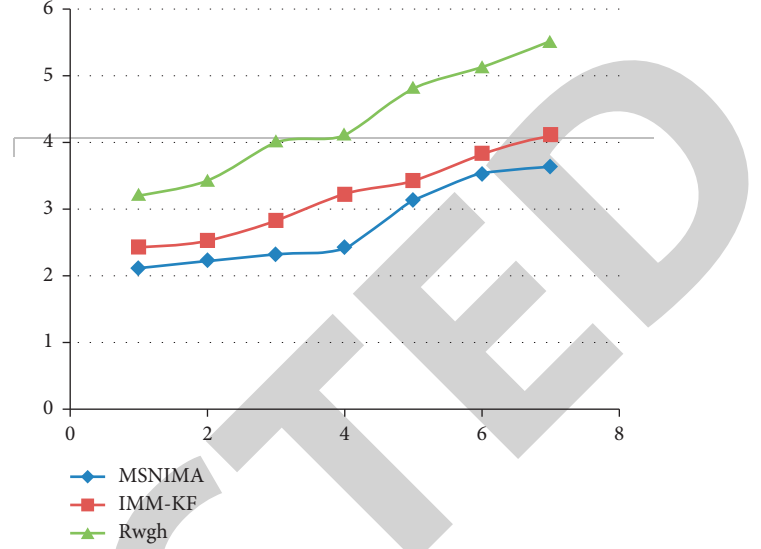


FIGURE 4: The relationship between LOS error variance σ_N^2 and RMSE.

Gaussian distribution, and the nonline-of-sight error variance affects the RMSE. From the results, as the value of σ_N^2 continues to increase, the corresponding RMSE calculation value of the algorithm also increases; the positioning performance of the MSNIMA algorithm is better than the other two algorithms, and it has the best positioning effect.

3.2.2. Nonline-of-Sight Error Obeys Exponential Distribution. As shown in Figures 5 and 6, the results are expressed as nonline-of-sight positioning obeys the corresponding exponential distribution. As shown in Figure 6, as the parameters continue to increase, the overall RMSE value shows a decreasing trend. Among them, the MSNIMA algorithm positioning accuracy is better than the other two algorithms and has obvious advantages.

As shown in Figure 6, the MSNIMA algorithm proposed in this paper is robust, and the positioning accuracy is significantly better than the other two algorithms, and the standard deviation of noise is small, and it has a higher positioning accuracy.

3.2.3. Nonline-of-Sight Error Obeys Uniform Distribution. The results between the maximum deviation coefficient U_{\max} and the root mean square error are shown in Figure 7. With the increase of the maximum deviation sparseness, the three algorithms all show an increasing trend, and the MSNIMA algorithm proposed in this paper has better positioning accuracy than the other 2 kinds.

The relationship between the noise standard deviation and the root mean square error of the smart mobile terminal is shown in Figure 8. The MSNIMA algorithm proposed in this paper is not sensitive to the measurement noise standard deviation, and the MSNIMA algorithm always maintains the best positioning effect.

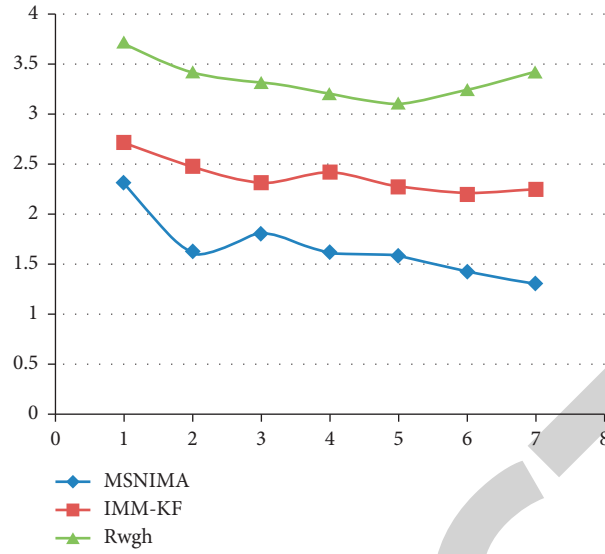


FIGURE 5: The relationship between parameter μ and RMSE.

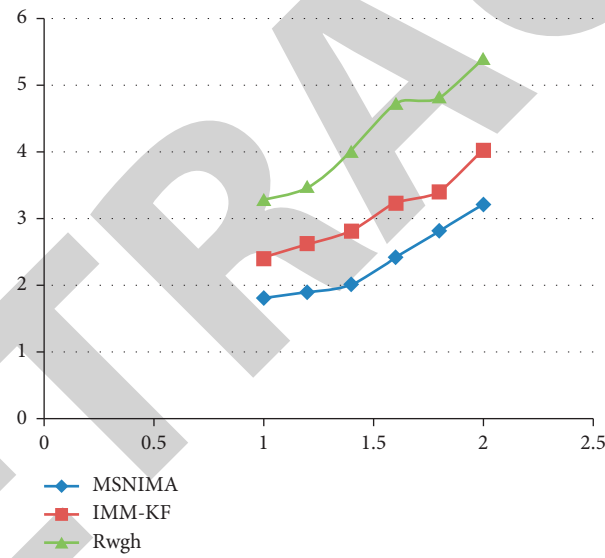


FIGURE 6: The relationship between the standard deviation of the measurement noise and the RMSE.

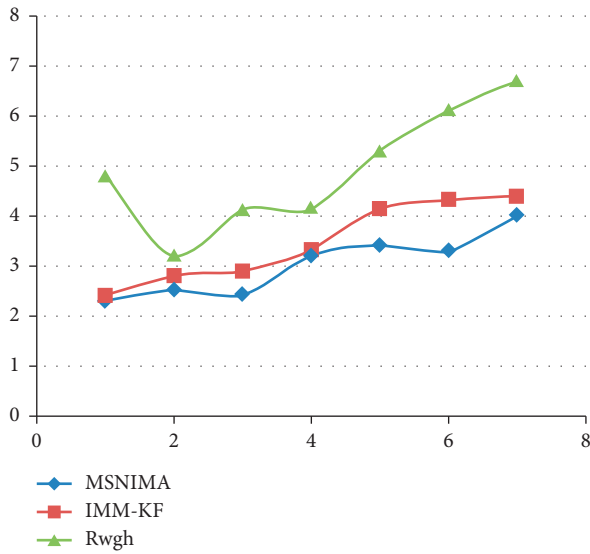


FIGURE 7: The relationship between U_{\max} and RMSE.

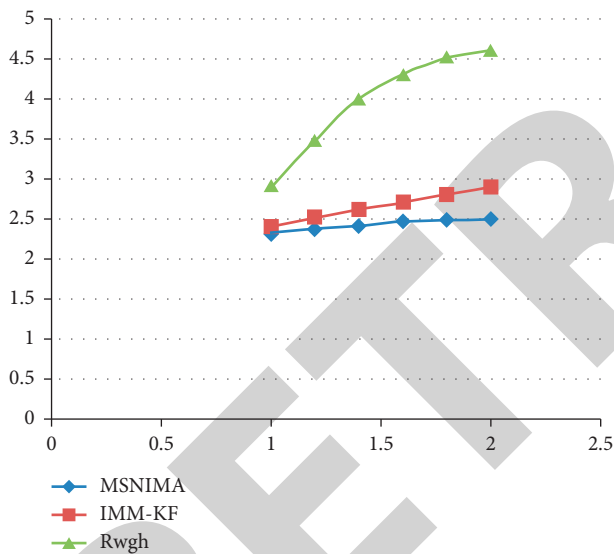


FIGURE 8: The relationship between the standard deviation of the measurement noise and the RMSE.

4. Conclusions

In response to the general demand for obtaining positioning, this article relies on the foundation of the multimedia sensor network intelligent monitoring architecture and proposes the MSNIMA positioning method, which comprehensively uses the radio frequency positioning function and the direction measurement function and simulates the direction of speed and movement. The corresponding positioning trajectory is calculated, and the corresponding errors are comprehensively considered to obtain the final high-precision positioning result. Simulation practice shows that MSNIMA can adapt to complex environments well and has achieved high positioning accuracy.

Data Availability

The data used to support the findings of this study are available from the author upon request.

Conflicts of Interest

The author declares no conflicts of interest.

References

- [1] S. Maiti, M. Mikami, and K. Hoshino, "Field experimental evaluation of mobile terminal velocity estimation based on Doppler spread detection for mobility control in heterogeneous cellular networks," *IEICE-Transactions on Communications*, vol. E100.B, no. 2, pp. 252–261, 2017.
- [2] Z. Y. Wu, M. Ismail, J. Kong, E. Serpedin, and J. Wang, "Channel characterization and realization of mobile optical wireless communications," *IEEE Transactions on Communications*, vol. 2, no. 9, pp. 1–8, 2020.
- [3] M. Alberti and M. L. Cour, "Face-down positioning versus non-supine positioning in macular hole surgery," *British Journal of Ophthalmology*, vol. 7, no. 4, pp. 109–117, 2015.
- [4] K. Ntontin and C. Verikoukis, "Toward the performance enhancement of microwave cellular networks through THz links," *IEEE Transactions on Vehicular Technology*, vol. 2, no. 7, pp. 1–8, 2017.
- [5] S. Yousefi, X.-W. Chang, and B. Champagne, "Mobile localization in non-line-of-sight using constrained square-root unscented kalman filter," *IEEE Transactions on Vehicular Technology*, vol. 64, no. 5, pp. 2071–2083, 2015.
- [6] N. B. Hassan, Z. Ghassemlooy, S. Zvanovec, P. Luo, and H. Le-Minh, "Non-line-of-sight $2 \times N$ indoor optical camera communications," *Applied Optics*, vol. 3, no. 2, pp. 104–110, 2018.
- [7] A. Mukherjee, P. Goswami, and A. Datta, "HML-based smart positioning of fusion center for cooperative communication in cognitive radio networks," *IEEE Communications Letters*, vol. 20, no. 11, pp. 2261–2263, 2016.
- [8] E. C. Kara, J. C. Macdonald, D. Black, M. Bérge, G. Hug, and K. Sila, "Estimating the benefits of electric vehicle smart charging at non-residential locations: a data-driven approach," *Applied Energy*, vol. 2, no. 1, pp. 98–103, 2015.
- [9] Y. Li, L. Liu, W. Ji, H. Peng, R. Zhao, and X. Zhang, "Strategies and materials of "SMART" non-viral vectors: overcoming the barriers for brain gene therapy," *Nano Today*, vol. 35, no. 3, pp. 101–106, 2020.
- [10] W. Liu, X. Shi, F. Zhu, X. Tao, and F. Wang, "Quality analysis of multi-GNSS raw observations and a velocity-aided positioning approach based on smartphones," *Advances in Space Research*, vol. 63, no. 8, pp. 2358–2377, 2019.
- [11] H. Hendrik, K. Zakaria, N. Abdelmoumen, and A. Eichhorn, "Accurate 3D positioning for a mobile platform in non-line-of-sight scenarios based on IMU/magnetometer sensor fusion," *Sensors*, vol. 18, no. 2, pp. 126–132, 2018.
- [12] B. Xie, D. Fang, T. Xing et al., "FISCP: fine-grained device-free positioning system for multiple targets working in sparse deployments," *Wireless Networks*, vol. 3, no. 1, pp. 1009–1014, 2016.
- [13] K.-H. Lee, D.-H. Jang, S.-J. Lee, and J.-R. Cha, "Target BER selection scheme in LMS networks using AL-FEC systems," *Computer Networks*, vol. 127, no. 3, pp. 190–199, 2017.
- [14] G. Retscher, J. Kleine, and L. Whitmore, "Trilateration approaches for seamless out-/indoor GNSS and Wi-Fi

- smartphone positioning,” *Journal of Applied Geodesy*, vol. 13, no. 1, pp. 47–61, 2019.
- [15] G. Retscher, J. Kleine, and L. Whitmore, “Trilateration approaches for seamless out-/indoor GNSS and Wi-Fi smartphone positioning,” *Journal of Applied Geodesy*, vol. 13, no. 4, pp. 1009–1014, 2018.

RETRACTED